Journal of Modern Optics
Vol. 56, No. 14, 10 August 2009, 1626–1631

Taylor & Francis
Taylor & Francis Group

Practical formula for the evaluation of high-order multiphoton absorption in thin nonlinear media

Juan J. Miret[a]*, María T. Caballero[a], Vicente Camps[a] and Carlos J. Zapata-Rodríguez[b]

[a]*Departamento de Óptica, Universidad de Alicante, P.O. Box 99, Alicante, Spain;*
[b]*Departamento de Óptica, Universidad de Valencia, Dr. Moliner 50, 46100 Burjassot, Spain*

(*Received 21 May 2009; final version received 29 July 2009*)

We present an analytical formula for the fast and accurate evaluation of nonlinear absorption in materials exhibiting an admixture of different multiphoton processes. This approach is specifically addressed for its use in thin films when the slowly varying envelope approximation applies. The contribution of absorptions of distinct order is conveniently averaged in order to use well-known expressions for a single multiphoton process. In the latter case, therefore, our simple expression is reduced toward the exact solution.

Keywords: nonlinear absorption; multiphoton absorption; nonlinear beam shaping

1. Introduction

Multiphoton absorption of intense wavefields in matter is a phenomenon of interest in a great variety of applications. In multiphoton microscopy, for example, enhanced optical sectioning is achieved leading to superresolved three-dimensional imaging without the use of a confocal aperture [1,2]. In this case, higher order nonlinear absorption (NLA) processes are mostly proposed to further improve spatial resolution and light penetration [3,4]. In optical limiting, on the other hand, highly nonlinear absorbing materials are also expected to exhibit large transmittance at low intensities, resistance to laser-induced damage, stability over time, and ultrafast responses [5,6].

The evaluation of multiphoton absorption in nonlinear flat films is accurately performed within the slowly varying envelope approximation [7]. This is of practical interest for instance in pursuit of characterizing the nonlinear response of a material, where the open aperture *Z*-scan provides the standards to determine the multiphoton absorption coefficients [8]. The analysis is carried out in a simple manner since the propagation of the electric field in the nonlinear medium is described by means of a differential equation having an analytical solution [9,10]. When more than one nonlinear process is active, however, the corresponding solution has not been reported to the knowledge of the authors. Interestingly, different approximate formulae considering linear absorption, two-photon absorption, and third-order nonlinear absorption, have recently been given elsewhere [11,12].

Let us point out that this is not a purely academic problem. For instance, ultrashort pulse propagation at 1320 nm in polydiacetylene-PTS exhibits simultaneous 2PA (two-photon absorption) and 3PA [13]. Also, an exact degeneracy between three- and four-photon absorption is observed at the peak wavelength of 1890 nm. In chalcogenide glasses, there is found an important contribution of 2PA in measuring the three-photon NLA coefficient at 1.06 μm in the picosecond range [11,14]. Even four- and five-photon absorption is observed in TeO_2-based samples at a wavelength of 1550 nm with a small linear absorption coefficient [15].

In this paper we address the problem of determining in a fast and clear way the laser beam shaping in passing through a thin slab of a nonlinear material, driven by an admixture of two different multiphoton processes of any order. In such a complex nonlinear material, we may identify and separate accurately the contribution of each multiphoton process to the field absorption within the slowly varying envelope approximation. Additionally, practical implementation of the derived formula is demonstrated in the computation of open aperture *Z*-scan traces.

2. Nonlinear absorption in a thin film

Let us consider a pulsed beam propagating in air along the z axis and impinging normally onto a thin bulk medium to prove its response upon NLA. In this study we assume that if the beam intensity is low enough to neglect NLA in the sample, the transverse profile is not

*Corresponding author. Email: jjmiret@ua.es

ISSN 0950–0340 print/ISSN 1362–3044 online

DOI: 10.1080/09500340903230015
http://www.informaworld.com

disturbed significantly due to diffraction. In this case the slowly varying envelope approximation applies [7]. Exceptionally, linear absorption in the thin sample is regarded. Now the intensity is governed by the simple equation:

$$\frac{\mathrm{d}I}{\mathrm{d}z} = -\alpha(I)I, \tag{1}$$

where z is the propagation depth within the nonlinear sample, and the intensity-dependent absorption

$$\alpha = \alpha_1 + \alpha_2 I + \alpha_3 I^2 + \alpha_4 I^3 + \cdots, \tag{2}$$

includes a linear term, α_1 (also denoted as α_0 elsewhere [10] or simply α), and nonlinear terms, α_n (for integers $n \geq 2$). Here we consider ultrashort pulse excitations so that slow (cumulative) nonlinearities such as thermal nonlinearity are ignored [16,17].

Let us first examine m-photon absorption and l-photon absorption simultaneously, being $2 \leq m, l$. Starting from the slowly varying envelope approximation we may simplify the evaluation of the field observed at the exit plane by means of the following differential equation

$$\partial_{\zeta_m} \tilde{I} = -\tilde{I}^m - \eta_{ml} \tilde{I}^l \tag{3}$$

and the contour condition $\tilde{I} = 1$ at $\zeta_m = 0$. We point out that a linear absorption process may be included in Equation (3) if $l = 1$ (or $m = 1$) and, alternatively, if we insert the term $-\eta_{m1}\tilde{I}$ on the right-hand side of the equation, cases that are considered below. Here, $\tilde{I} = I/I_0$ stands for the ratio of the output intensity I and the input intensity I_0 in the sample, the reduced axial coordinate $\zeta_m = z/L_m$ is the ratio of the sample depth z and the characteristic length for the m-photon absorption process,

$$L_m = \frac{1}{\alpha_m I_0^{m-1}}, \tag{4}$$

being α_m the m-photon nonlinear absorption coefficient. For instance, in polydiacetylenes typically [13] $\alpha_2 = 6\,\mathrm{cm\,GW^{-1}}$ and $\alpha_3 = 2.7\,\mathrm{cm^3\,GW^{-2}}$ at 1320 nm so that $L_2 = 830\,\mu\mathrm{m}$ and $L_3 = 930\,\mu\mathrm{m}$ for a peak intensity $I_0 = 2\,\mathrm{GW\,cm^{-2}}$. Finally,

$$\eta_{ml} = \frac{L_m}{L_l} = \frac{\alpha_l}{\alpha_m} I_0^{l-m} \tag{5}$$

represents the relative strength of both NLA processes. In our numerical example $\eta_{23} = 0.9$ suggesting a balanced charge of both nonlinear phenomena.

The permutation $m \leftrightarrow l$ in (3) provides an equivalent form of the differential equation; if one combination shows $\eta_{ml} \geq 1$ the counterpart gives $\eta_{lm} = \eta_{ml}^{-1} \leq 1$. We may restrict our problem considering mPA a dominant process over lPA, whence leaving the unity as the maximum value of the coupling parameter η_{ml}. According to Equation (5), $\eta_{ml} \leq 1$ at sufficiently low intensities if $m < l$.

Validity of Equation (3) is restricted to nonlinear interactions with matter producing small and modest alterations of the beam profile. Otherwise, multiphoton absorption may lead to self-focusing within the sample. In mathematical terms we impose $\zeta_m |\partial_{\zeta_m} \tilde{I}| \ll \tilde{I}$. Using Equations (4) and (5) we infer a sufficient condition $z \ll L_n$ (or $\zeta_n \ll 1$) for $n = m, l$.

In general, one cannot find an analytical solution of Equation (3). For a single NLA process being $\eta_{ml} = 0$, a solution may be provided in a closed form. In this case, Equation (3) is reduced to $\partial_{\zeta_m} \tilde{I} = -\tilde{I}^m$, and the exit intensity in the medium yields

$$\tilde{I} = \frac{1}{[1 + (m-1)\zeta_m]^{1/(m-1)}}. \tag{6}$$

In some circumstances, e.g. $(m-1)\zeta_m \geq 1$, Equation (6) provides a significant beam depletion due to strong m-photon absorption, a result that is not valid in our approach. Therefore, we focus our attention on the regime $\zeta_m \ll 1$. In this case we may expand Equation (6) into a Taylor series around $\zeta_m = 0$ giving

$$\tilde{I}^{(S)} = 1 + \sum_{s=1}^{S} \frac{\zeta_m^s}{s!} \prod_{p=0}^{s-1} [p - pm - 1] + O[\zeta_m]^{S+1}, \tag{7}$$

where S is a positive integer. In the limit $S \to \infty$, $I^{(\infty)}$ provides an exact solution of the transmitted field intensity. We point out that $\zeta_m = 0$ stands for sufficiently thin samples but also for sufficiently low input intensities such that NLA of m photons is negligible, in accordance with the definition $\zeta_m = \alpha_m z I_0^{m-1}$. Specifically $\tilde{I}^{(1)} = 1 - \zeta_m$, and the parabolic approximation yields

$$\tilde{I}^{(2)} = \tilde{I}^{(1)} + \frac{m}{2}\zeta_m^2 = 1 - \zeta_m + \frac{m}{2}\zeta_m^2, \ (\eta_{ml} = 0). \tag{8}$$

Interestingly, we may provide a solution of the more complex Equation (3) also in terms of polynomials of ζ_m. We point out that a different approach using the method of Adomian may provide an approximate solution of (3) given also in terms of a series expansion [12,18]. Developing $\tilde{I}$ into a Taylor series about the origin, the first-order solution yields

$$\tilde{I}^{(1)} = \tilde{I}_0 + (\partial_{\zeta_m} \tilde{I})_0 \zeta_m = 1 - (1 + \eta_{ml})\zeta_m, \tag{9}$$

where subindex 0 stands for the specific value at $\zeta_m = 0$. Equations (7) for $S = 1$ [also shown in (8)] and (9) are formally equivalent within this linear approach; however, for simultaneous NLA processes we use $(1 + \eta_{ml})\zeta_m$ instead of ζ_m. In this context we interpret

that, in a low-order approximation, our solution for competing NLAs might correspond to the solution for a single one with $\zeta_m \to \zeta_{ml} = z/L_{ml}$ and characteristic absorption depth L_{ml}, satisfying

$$\frac{1}{L_{ml}} = \frac{1}{L_m} + \frac{1}{L_l}. \tag{10}$$

The average length L_{ml} approaches L_m in the low-intensity regime where $L_m \ll L_l$, but shifts toward L_l as long as the input intensity increases. In general, since two NLA processes are present, L_{ml} is lower than either L_m or L_l individually. The quadratic (second-order) approximation obtained from the Taylor series yields

$$\tilde{I}^{(2)} = \tilde{I}^{(1)} + \frac{(1+\eta_{ml})(m+l\eta_{ml})}{2}\zeta_m^2. \tag{11}$$

We point out that the last term of the polynomial expansion is evaluated using the chain rule

$$\partial^2_{\zeta_m} \tilde{I} = \partial_{\tilde{I}}(\partial_{\zeta_m}\tilde{I})\partial_{\zeta_m}\tilde{I} \tag{12}$$

and Equation (3). Once again, Equation (11) would be associated with beam depletion under a single NLA process [see (8)] in using the axial coordinate $(1+\eta_{ml})\zeta_m$, as previously discussed within the linear approximation, and also substituting the number m of photons by the average

$$\bar{m} = \left(\frac{L_{ml}}{L_m}\right)m + \left(\frac{L_{ml}}{L_l}\right)l = \frac{m+l\eta_{ml}}{1+\eta_{ml}}. \tag{13}$$

This parameter spans from m to l as η_{ml} moves from zero ($L_m \ll L_l$) to infinity ($L_m \gg L_l$). We point out that the weight of each order [i.e. (L_{ml}/L_m) for the order m] varies from zero to the unit, and the sum of all of them obviously gives

$$\left(\frac{L_{ml}}{L_m}\right) + \left(\frac{L_{ml}}{L_l}\right) = 1. \tag{14}$$

Moreover, $\bar{m}$ stands for the arithmetic mean of m and l at balanced lengths $L_m = L_l$ ($\eta_{ml} = 1$).

Solution of Equation (3) is computed numerically and represented graphically in Figure 1 for different values of m and l. A unit value of η_{ml} is selected in order to analyze NLAs with balanced strengths within the sample. The linear approach given in (9) overestimates field attenuation due to absorption, whereas the quadratic approximation (11) underestimates it. The validity of these approximations is restricted to low depths, $\zeta_m \ll 1$, and deviations upon the exact solution become severe if ζ_m approaches unity. Though not represented in the figure, convergence with higher-order solutions gives results that are extremely slow, showing strong oscillations upon the order S of the

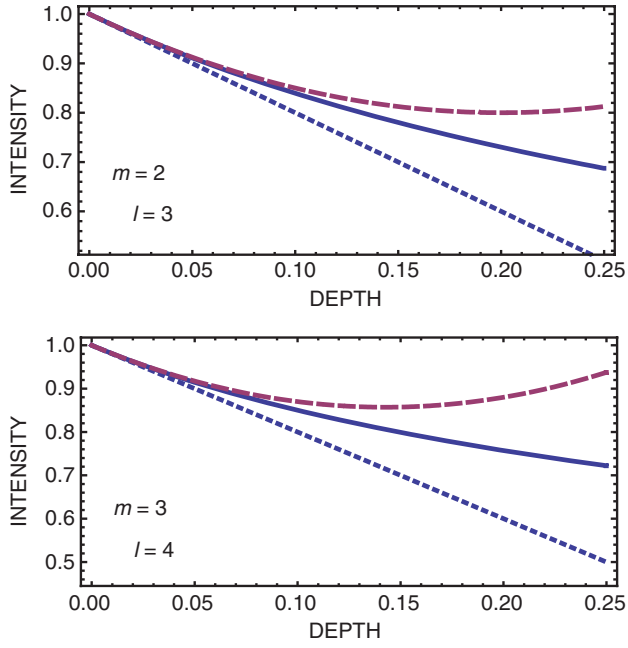

Figure 1. Evolution of $\tilde{I}$ when mPA and lPA are present simultaneously. Depth ζ_m is in the horizontal axis and the parameter $\eta_{ml} = 1$. Numerical evaluation of (3) is plotted with solid lines. Also, the linear approximation (9) is drawn with dotted lines, and $I^{(2)}$ of Equation (11) is represented by dashed lines. (The color version of this figure is included in the online version of the journal.)

approach if $\zeta_m \lesssim 1$. This suggests that a Fourier expansion in terms or harmonic functions could be more convenient than a Taylor series of polynomials. Nevertheless, we follow a different approach next.

Let us exploit the fact that beam depletion under simultaneous mPA and lPA behaves similarly to single $\bar{m}$PA, for which the exact solution (6) might be provided. Hence, using the axial coordinate ζ_{ml} instead of ζ_m in Equation (6), and substituting the number m of photons absorbed in the process by the average $\bar{m}$ given in (13), we finally have

$$\tilde{I} \approx \frac{1}{[1+(\bar{m}-1)\zeta_{ml}]^{1/(\bar{m}-1)}}, \tag{15}$$

where $\zeta_{ml} = z/L_{ml}$, that is, $\zeta_{ml} = (1+\eta_{ml})\zeta_m$. In the limit $\eta_{ml} = 0$, obviously, Equation (15) simplifies to Equation (6) giving the exact solution.

In Figure 2 we inspect graphically the accuracy of (15) for the intermediate value $\eta_{ml} = 1$. Within the interval of interest, $0 \le \zeta_m \le 1$, deviations of the computed intensities and those available from Equation (15) have the upper bound 9.7×10^{-3} found at $\zeta_2 = 1$ for mixed 2PA and 3PA processes, representing a relative error of less than 1%. For simultaneous 3PA and 4PA, accuracy improves since deviation decreases to 5.1×10^{-3} at $\zeta_3 = 1$.

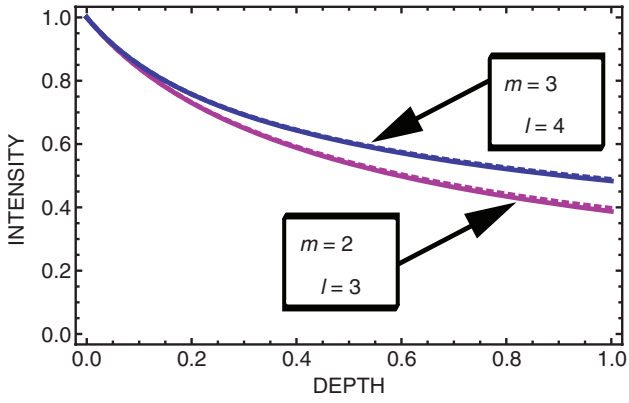

Figure 2. Behavior of $\tilde{I}$ within depths $\zeta_m \leq 1$, assuming mPA and lPA occur at $\eta_{ml}=1$. Numerical evaluation of (3) is plotted with solid lines. Also, the analytical approach given in (15) is drawn with dotted lines. (The color version of this figure is included in the online version of the journal.)

3. Samples with strong linear absorption

Literature values for the linear-optical absorption coefficient α_1 in the near-infrared region vary between 0.1 and 100 cm^{-1} for PTS [19], the example given above, giving characteristic lengths as short as $L_1 = 100\,\mu\mathrm{m}$. Linear absorption dominates over NLA processes at sufficiently low values of I_0 and therefore, such an effect cannot be neglected in this regime. In this sense, a solution of Equation (3) may be provided for $l=1$, that is, when linear absorption and only a single nonlinear process is active, which is written as [9,14]

$$\tilde{I} = \frac{\exp(-\eta_{m1}\zeta_m)}{[1+(m-1)\zeta_{\mathrm{eff}m}]^{1/(m-1)}}. \tag{16}$$

Here,

$$\zeta_{\mathrm{eff}m} = \frac{1-\exp[-(m-1)\eta_{m1}\zeta_m]}{(m-1)\eta_{m1}} \tag{17}$$

stands for the effective axial coordinate. Importantly, the product $\eta_{m1}\zeta_m$ ($\triangleq\zeta_1$) is independent of L_m. Also, $\zeta_{\mathrm{eff}m}$ and Equation (16) lead to ζ_m and Equation (6), respectively, if $\eta_{m1}=0$.

The analyticity of solution (16) suggests that an approach of $\tilde{I}$ may be given for the complete equation

$$\partial_{\zeta_m}\tilde{I} = -\eta_{m1}\tilde{I} - \tilde{I}^m - \eta_{ml}\tilde{I}^l, \tag{18}$$

which accounts for linear absorption and two different NLA processes, simultaneously. Accordingly, we may follow the procedure given above identifying the terms in the parabolic series expansion of $\tilde{I}$ about the origin, $\zeta_m=0$, derived here from Equation (16) as

$$\tilde{I} \approx 1 - (1+\eta_{m1})\zeta_m + \frac{(1+\eta_{m1})(m+\eta_{m1})}{2}\zeta_m^2, \tag{19}$$

and also from Equation (18) giving

$$\tilde{I} \approx 1 - (1+\eta_{m1}+\eta_{ml})\zeta_m + \frac{(1+\eta_{m1}+\eta_{ml})(m+\eta_{m1}+l\eta_{ml})}{2}\zeta_m^2. \tag{20}$$

Using over Equation (19) [and Equation (16)] the normalization of the axial coordinate $\zeta_m \to \zeta_{ml} = z/L_{ml}$ in terms of the average length of Equation (10), and also substituting the number m of photons by the average $\bar{m}$ of (13), lead to severe simplifications as $m\zeta_m \to \bar{m}\zeta_{ml} = (m+l\eta_{ml})\zeta_m$ [and trivially $\zeta_m \to (1+\eta_{ml})\zeta_m$]. The required approach is straightforwardly attained if we additionally substitute $\eta_{m1} = L_m/L_1$ by

$$\eta_{\bar{m}1} = \frac{L_{ml}}{L_1}, \tag{21}$$

allowing the conservation of the coordinate $\zeta_1 = \alpha_1 z$, i.e. $\eta_{m1}\zeta_m = \eta_{\bar{m}1}\zeta_{ml}$. Based upon the averages introduced above, we may recast Equation (16) as

$$\tilde{I} = \frac{\exp(-\zeta_1)}{[1+(\bar{m}-1)\zeta_{\mathrm{eff}\bar{m}}]^{1/(\bar{m}-1)}}, \tag{22}$$

to account for different NLA processes. The formula shown in Equation (22) is the main result presented in this paper. The effective axial coordinate

$$\zeta_{\mathrm{eff}\bar{m}} = \frac{1-\exp[-(\bar{m}-1)\zeta_1]}{(\bar{m}-1)\eta_{\bar{m}1}}, \tag{23}$$

also has been transformed conveniently from (17) by using the average $\bar{m}$ and $\eta_{\bar{m}1}$ instead of the integer m and η_{m1}, respectively.

Validity of Equation (22) is examined in Figure 3 for balanced absorption processes, i.e. $\eta_{ml}=1$ and $\eta_{m1}=1$. Numerical simulations are also depicted, and an excellent agreement with Equation (22) is remarkable. We point out that approach (22) provides the exact value of $\tilde{I}$ in the limits $\eta_{ml}=0$, $\eta_{m1}=0$, $\eta_{ml}\to\infty$, and $\eta_{m1}\to\infty$.

4. Application to the evaluation of *Z*-scan traces

From an experimental point of view, nonlinear samples are commonly proved with paraxial Gaussian beams focused with low-numerical-aperture lenses. Top-hat beams and trimmed Airy beams are claimed to present some advantages over Gaussian beams for Z-scan experiments [20]; however, beam shaping of the laser beam is required. Also, Gaussian beams are found to be more attractive in theoretical studies because the three-dimensional distribution of the field is an analytic solution of the paraxial wave equation [21]. In this study we assume a sufficiently narrow bandwidth of

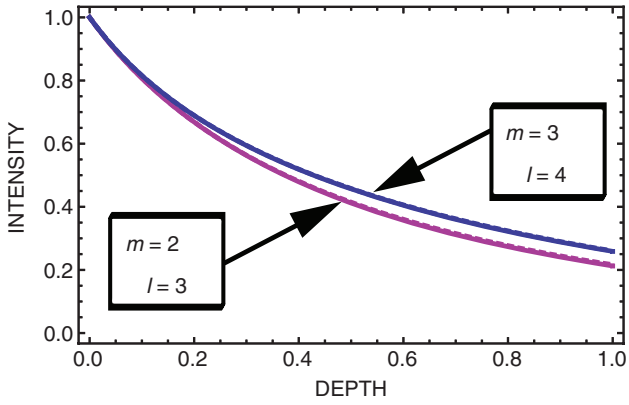

Figure 3. Dependence of $\tilde{I}$ at different depths when mPA, lPA, and linear absorption are found simultaneously at $\eta_{ml}=1$ and $\eta_{m1}=1$. Again, the numerical estimation of $\tilde{I}$ is plotted with solid lines, and the approximation given in (22) is drawn with dotted lines. (The color version of this figure is included in the online version of the journal.)

the pulsed wave in order to neglect spatiotemporal couplings associated with ultrafast beam propagation [22,23]. For convenience, we use normalized spatial coordinates: the radial coordinate r involves a normalization with respect to the beam waist w_0 and the axial coordinate z is given in units of the Rayleigh range $z_R = kw_0^2/2$, $k=\omega/c$ being the wavenumber in air. If the waist plane of the Gaussian beam is found at $z=0$ (neglecting focal shifts [24], this is the focal plane of the lens), the instantaneous intensity at the input plane of the scanned sample yields

$$I_0(r,z,t) = E(t)w^{-2}\exp\left(-2r^2/w^2\right), \tag{24}$$

with

$$w(z) = (1+z^2)^{1/2} \tag{25}$$

being the Gaussian width, and $E(t)$ the intensity of the pulse envelope at focus, $(r,z)=(0,0)$. The temporal coordinate t supports a normalization over the pulse duration such that

$$\frac{1}{E_0}\int_{-\infty}^{\infty} \mathrm{d}t E(t) = 1, \tag{26}$$

where E_0 is the maximum instantaneous intensity. For the sake of convenience, from hereon we consider pulse waveforms with a Gaussian profile. In this case we write $E(t)=E_0\exp(-\pi t^2)$ so that its FWHM yields $\Delta\tau = 2(\ln 2/\pi)^{1/2}\approx 0.94$. We point out that our analysis may be extended to other waveforms straightforwardly.

In the open-aperture mode of Z-scan measurements, light transmitted through the sample is fully collected. Mismatching of the linear index of refraction of the sample and air induces the incident beam to be partially reflected, an effect that may be treated in the experimental data and is therefore ignored here. The output intensity $I=I_0\tilde{I}$ is obtained from Equations (22) and (24), which varies in space and time. For a thin nonlinear material of width L, the coordinate ζ_m reaches a maximum value

$$\Delta_m = \alpha_m L E_0^{m-1} \tag{27}$$

at focus. Also the coupling parameter satisfies $\eta_{ml}\leq \Delta_l/\Delta_m$ (if $m<l$). Upon recording of the integrated intensity at the exit plane of the scanned sample,

$$P(z) = \int_{-\infty}^{\infty}\mathrm{d}t\int_0^{\infty} 2\pi r\mathrm{d}r I(r,z,t), \tag{28}$$

changes are found in the vicinity of the Gaussian focus, $|z|<1$. In the far-field, $|z|\gg 1$, the output intensity $I\to I_0\exp(-\Delta_1)$ so that Equation (28) yields

$$P_\infty = \lim_{z\to\infty} P(z) = \frac{\pi}{2}E_0\exp(-\Delta_1). \tag{29}$$

Commonly, Z-scan signatures refer to traces of the ratio $T=P/P_\infty$, which is interpreted as the normalized transmittance of the sample as being scanned axially. We point out that the use of Equation (22) to track the Z-scan trace leads to an ordinary numerical integration.

In order to simplify our discussion for the remainder of Section 4, let us neglect linear absorption by using the limit $\Delta_1\to 0$. In Figure 4 we depict Z-scan signatures when the sample experiences 2PA and 3PA simultaneously (subfigure on the left), and when 3PA and 4PA are present (on the right). The strength of each NLA process is characterized by the corresponding parameters Δ_m and Δ_l. Numerical simulations of the transmittance T are performed using the approximated Equation (22) [also Equation (15)]; we have observed by direct comparison with numerical computation of Equation (3) that these traces are of extremely high accuracy for low and intermediate values of Δ_m and Δ_l. Specifically, Z-scan responses are symmetric even functions with respect to the origin, $z=0$. As expected, NLA is maximum at the Gaussian focus. Moreover, the V-shaped response T shows a distinct tail decay and valley value, a fact that may be employed to determine NLA coefficients of the sample from experimental data [10].

5. Conclusions

In this paper we have derived a simple formula, Equation (22), to use deductively when multiphoton absorption of different nature arise simultaneously. When a single nonlinear process governs the wave propagation, Equation (22) gives the solution of the

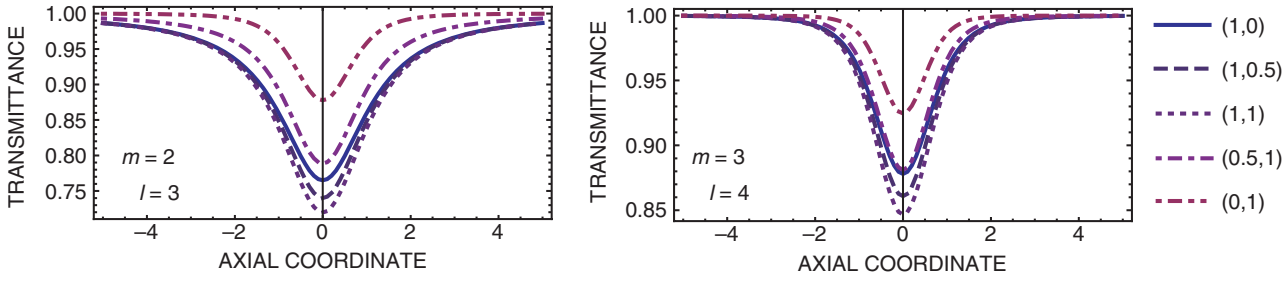

Figure 4. *Z*-scan signatures for 2PA and 3PA admixes (left) and simultaneous 3PA and 4PA processes (right). Dominant *m*PA with $\Delta_m = 1$ (and $\Delta_l = 0$) is drawn with solid line. Other values of the ordered pair (Δ_m, Δ_l) are represented by different curve styles. (The color version of this figure is included in the online version of the journal.)

intensity evolution in the SVEA. As a particular feature, it is expressed in terms of a characteristic length L_m, which is inversely proportional to the *m*-photon nonlinear absorption coefficient, and the number m of photons involved in the nonlinear process. Our approach consists of the parametrization of the nonlinear beam propagation, which is formulated in terms of a polynomial series expansion. In the general case, simple rules are disclosed for the average of L_m and m of the different high-order nonlinear absorption processes that are considered. Thus, the relevancy of our method lies in taking a well-known expression and making it have general application.

Finally, we have put Equation (22) serving a utilitarian purpose. Specifically, we have demonstrated fast and accurate computation of open aperture Z-scan signatures. In this case, an ordinary numerical integration leads to the trace tracking. Numerical simulations are presented for 2PA and 3PA admixes, and also for simultaneous 3PA and 4PA processes.

Acknowledgements

The authors are indebted to Florencio E. Hernandez for stimulating conversations. This research was funded by Ministerio de Ciencia e Innovación (MICIIN) and Generalitat Valenciana under the projects TEC2009-11635 and GVPRE/2008/005, respectively. CJZR personally acknowledges financial support from MICIIN.

References

[1] Denk, W.; Strickler, J.H.; Webb, W.W. *Science* **1990,** *248,* 73–76.
[2] Gu, M. *Opt. Lett.* **1996,** *21,* 988–990.
[3] Larson, D.R.; Zipfel, W.R.; Williams, R.M.; Clark, S.W.; Bruchez, M.P.; Wise, F.W.; Webb, W.W. *Science* **2003,** *300,* 1434–1436.
[4] Polesana, P.; Faccio, D.; Trapani, P.D.; Dubietis, A.; Piskarskas, A.; Couairon, A.; Porras, M. *Opt. Express* **2005,** *13,* 6160–6167.
[5] Van Stryland, E.W.; Vanherzeele, H.; Woodall, M.A.; Soileau, M.J.; Smirl, A.L.; Guha, S.; Boggess, T.F. *Opt. Eng.* **1985,** *24,* 613–623.
[6] Venkatram, N.; Rao, D.N.; Akundi, M.A. *Opt. Express* **2005,** *13,* 867–872.
[7] Shen, Y.R. *Nonlinear Optics*; Wiley: New York, 1984.
[8] Sheik-Bahae, M.; Said, A.A.; Wei, T.; Hagan, D.; Van Stryland, E.W. *IEEE J. Quantum Electron.* **1990,** *26,* 760–769.
[9] Hermann, J.A. *J. Opt. Soc. Am. B* **1984,** *1,* 729–736.
[10] Corrêa, D.S.; Boni, L.D.; Misoguti, L.; Cohanoschi, I.; Hernandez, F.E.; Mendonça, C.R. *Opt. Commun.* **2007,** *277,* 440–445.
[11] Boudebs, G.; Cherukulappurath, S.; Guignard, M.; Troles, J.; Smektala, F.; Sanchez, F. *Opt. Commun.* **2004,** *232,* 417–423.
[12] Sanchez, F.; Leblond, H.; Brunel, M.; Ameur, K.A. *J. Nonlinear Opt. Phys. Mater.* **2006,** *15,* 219–225.
[13] Yoshino, F.; Polyakov, S.; Liu, M.; Stegeman, G. *Phys. Rev. Lett.* **2003,** *91,* 063902.
[14] Cherukulappurath, S.; Godet, J.L.; Boudebs, G. *J. Nonlinear Opt. Phys. Mater.* **2005,** *14,* 49–60.
[15] Bindra, K.S.; Bookey, H.T.; Kar, A.K.; Wherrett, B.S.; Liu, X.; Jha, A. *Appl. Phys. Lett.* **2001,** *79,* 1939–1941.
[16] Shinkawa, K.; Ogusu, K. *Opt. Express* **2008,** *16* (22), 18230–18240.
[17] Ogusu, K.; Shinkawa, K. *Opt. Express* **2008,** *16,* 14780–14791.
[18] Sanchez, F.; Abbaoui, K.; Cherruault, Y. *Opt. Commun.* **2000,** *173,* 397–401.
[19] Krug, W.; Miao, E.; Derstine, M.; Valera, J. *J. Opt. Soc. Am. B* **1989,** *6,* 726–732.
[20] Rhee, B.K.; Byun, J.S.; Stryland, E.W.V. *J. Opt. Soc. Am. B* **1996,** *13,* 2720–2723.
[21] Siegman, A.E. *Lasers*; University Science Books: Mill Hill Valley, CA, 1986.
[22] Porras, M.A. *Phys. Rev. E* **1998,** *58,* 1086–1093.
[23] Zapata-Rodríguez, C.J. *J. Opt. Soc. Am. A* **2007,** *24,* 675–686.
[24] Li, Y.; Wolf, E. *Opt. Commun.* **1981,** *39,* 211–215.